Cardiomyocyte Migration in Mammalian Heart Regeneration

Arnar Bragi Ingason

Thesis submitted towards Bachelor‘s degree in Science
University of Iceland
Faculty of Medicine
School of Health Sciences

HÁSKÓLI ÍSLANDS

Cardiomyocyte Migration in Mammalian Heart Regeneration

Arnar Bragi Ingason[1]

Thesis submitted in partial fulfillment of a
Baccalaureus Scientiarum degree

Supervisor(s):
Y. Joseph Woo, M.D.[2]
Andrew B. Goldstone, M.D.[2]

[1]Department of Medicine, University of Iceland
[2]Department of Cardiothoracic Surgery, Stanford University School of Medicine

University of Iceland
Faculty of Medicine
School of Health Sciences
Reykjavik, 2016

Stanford | MEDICINE

HÁSKÓLI ÍSLANDS

Thesis submitted in partial fulfillment of a *Baccalaureus Scientiarum* degree. Thesis may not be reproduced, in whole or in part, by any means, without the author's consent.

Table of Contents

Abstract

Introduction

Although heart regeneration in neonatal mice has been recently studied, the mechanism by which cardiomyocytes migrate to reconstitute the area of injury is unknown. Heart regeneration has been shown to depend upon both macrophage infiltration and angiogenesis. Furthermore, a study on nerve regeneration following resection showed that Schwann cells migrated along macrophage-directed blood vessels to bridge the gap between transected edges. We hypothesized that a similar mechanism might direct cardiomyocytes following apical resection.

Methods

Day 1 postnatal mice were subjected to either apical resection or sham surgery. Hearts were explanted at serial time points and examined with immunohistochemistry to visualize revascularization and cardiomyocyte migration into the region of resection. To address if cardiomyocytes migrate along endothelial cells, a transwell migration assay was performed whereby isolated cardiomyocytes and human umbilical vein endothelial cells were co-cultured and tracked using time-lapse microscopy.

Results

This study showed that angiogenesis precedes cardiomyocyte migration during mammalian heart regeneration. Cardiomyocyte processes – characteristic of cell migration – are typically in close proximity to nearby blood vessels regenerating region. Furthermore, when cardiomyocytes and HUVECs were co-cultured *in vitro*, the majority of the cardiomyocytes coaligned with the endothelial tubules.

Conclusion

The close proximity of migrating cardiomyocytes to blood vessels both *in vivo* and *in vitro* suggests a close relationship between the two cell types. Further verification is needed to conclude whether capillaries are necessary and sufficient to direct cardiomyocyte migration.

Útdráttur

Inngangur

Þrátt fyrir að endurnýjun hjartans í nýfæddum músum hafi verið nýlega rannsakað er enn óljóst hvernig skrið hjartavöðvafruma til blóðtappasvæðis fer fram eftir brottnám hjartabrodds. Sýnt hefur verið að endurnýjun hjartans er háð bæði ígöngu makrófaga og nýæðamyndunar. Enn fremur hefur rannsókn á endurnýjun úttaugar sýnt að eftir að settaug er klippt í tvennt berast makrófagar í bilið og örva nýæðamyndun í bilinu. Schwann frumur skríða svo eftir þessum æðum og brúa bilið milli klipptu endanna. Við settum því fram þá tilgátu að skrið hjartavöðvafruma fylgi svipuðu ferli eftir brottnám hjartabrodds.

Aðferðir

Eins dags gamlar mýs voru annað hvort meðhöndlaðar með hjartabroddsbrottnámi eða sham aðgerð. Mótefnalitanir voru síðan gerðar á mismunandi tímapunktum til þess að skoða skrið æðaþels- og hjartavöðvafruma til blóðtappasvæðis. Til þess að meta hvort hjartavöðvafrumur skríða eftir æðaþeli var svokölluð *transwell migration assay* framkvæmd þar sem hjartavöðvafrumur og mennskar naflastrengsbláæðaþelsfrumur voru ræktaðar saman og myndir teknar á smásjá á tíu mínútna fresti yfir 12 klst tímabil.

Niðurstöður

Niðurstöður sýndu að blóðæðar bárust inn í blóðtappasvæði á undan hjartavöðvafrumum. Meirihluti útskota skríðandi hjartavöðvafruma var auk þess í nálægð við blóðæðar í blóðtappasvæði. Loks lágu flestar hjartavöðvafrumur samhliða æðaþelsneti þegar frumutegundirnar tvær voru ræktaðar saman.

Ályktanir

Nálægð skríðandi hjartavöðvafruma og blóðæða *in vivo* og *in vitro* bendir til þess að sterkt samband sé milli frumutegundanna tveggja. Frekari rannsóknir þarf hins vegar til þess að meta hvort æðaþelsfrumur séu nauðsynlegar og nægjanlegar til þess að stýra skriði hjartavöðvafruma.

List of Figures

Acknowledgments

I would like to thank my supervisors, Joseph Woo, M.D. and Andrew Goldstone, M.D., for allowing me the opportunity to come and work with them, for their mentorship, patience, and help. Additionally, I would like to thank my colleagues in Dr. Woo‘s laboratory for all of their help and support. I would like to thank Ruby Dewi from the Heilshorn Biomaterial group at Stanford University for her help in setting up the *in vitro* migration assays. Last but not least, I would like to thank Arnar Geirsson, M.D., for connecting me with Dr. Woo, and for invaluable advice preceding my exchange experience at Stanford. The project was performed within Dr. Woo’s laboratory in the Department of Cardiothoracic Surgery at Stanford University School of Medicine.

Abbreviations

C-14 = Carbon-14

ChIP seq = Chromatin immunoprecipitation sequencing

DAPI = 4',6-diamidino-2-phenylindole

DGC = Dystrophin glycoprotein complex

DLL4 = Delta-like canonical Notch ligand 4

DMEM = Dulbecco‘s Modified Eagle Medium

DNA = Deoxynucleic acid

EC = Endothelial cells

ECG = Electrocardiogram

ECM = Extracellular matrix

EdU = 5-Ethynyl-2-deoxyuridine

EPC = Endothelial progenerator cells

EphB2 = Ephrin receptor B2

FBS = Fetal bovine serum

FGF = Fibroblast growth gactor

GFP = Green Fluoroscent Protein

HBSS = Hanks’ balanced salt solution

HIF-1 = Hypoxia-inducible factor-1

HuR = Human antigen R

HUVEC = Human umbilical vein endothelial cell

IHC = Immunohistochemistry

LAD = Left anterior descending artery

MCP-1 = Monocyte chemoattractant protein 1

MI = Myocardial infarct

mi-R15 = MicroRNA 15

MMP = Matrix metalloprotease

NO = Nitric oxide

PAI-1 = Plasminogen activator inhibitor 1

PBS = Phosphate buffered saline

PBS-Tx = Phosphate buffered saline containing TritonX-100

PDGF-B = Platelet-derived growth factor B

RT-qPCR = Reverse transcriptase quantative polymerase chain reaction

SDF = Stromal-derived factor

SEM = Standard error of mean

SMC = Smooth muscle cells

TGFβ = Transforming growth factor β

TIMP = Tissue inhibitors of matrix metalloprotease

UNC5B = UNC5 Netrin Receptor B

VEGF = Vascular endothelial growth factor

VEGFR2 = Vascular endothelial growth factor receptor 2

VEGFR3 = Vascular endothelial growth factor receptor 3

YAP = Yes-associated protein

Introduction

Heart Regeneration

Hearts of lower vertebrates, such as zebra fish and newts, have been shown to have robust regenerative potential [1-3]. On the other hand, mammalian cardiomyocytes have long been considered to permanently exit the cell cycle shortly after birth with concurrent loss of proliferation; a process known as terminal differentiation. Further cardiac growth is therefore provided by hypertrophy and not hyperplasia [4].

Within the first week of life, mammalian cardiomyocytes begin duplicating their DNA and become binucleated [5]. Concurrently, the foramen ovale closes with septation [6]. Before this, the mammalian heart resembles the single circulation of the mononucleated hearts of adult zebrafish. This resemblance has led scientists to hypothesize that mammalian hearts have conserved regenerative potential in early life. In fact, recent findings suggest that neonatal mice regenerate their heart during their first week of life if exposed to injury in the form of apical resection or myocardial infarction [7, 8]. This "regenerative window" can be further prolonged to three weeks by miR-15 knockout [8].

Evidence suggests that human neonatal hearts may have similar regenerative potential. A recent publication reported a human who suffered from a myocardial infarct (MI) due to LAD occlusion at 1 day of life, recovered full cardiac function within 12 months of the event. The patient's serum markers of cardiac injury all declined rapidly to normal values after thrombolytic therapy [9]. Other case reports have described similar recovery after MI in neonates [10-15].

Conversely, evidence suggests that human adult hearts have limited regenerative potential. Using measurements of C-14 integration into DNA to determine cardiomyocyte age (C-14 accumulated in the atmosphere after atomic bomb experiments during the cold war), it has been concluded that annual cardiomyocyte renewal is approximately 1%/year at the age of 25, declining to 0.45%/year at the age of 75 [16]. Additionally, another investigation has shown a 3.4 fold increase in cardiomyocyte number between birth and age 20. Cardiomyocyte proliferation was greatest in infancy but remained evident after 40 years of age [17].

This renewal, however, is inadequate to compensate for lost myocardium following cardiac injury, thereby leading to scar tissue formation, adverse cardiac remodeling, and reduced ventricular function. If severe enough, an MI ultimately results in heart failure [18].

Heart transplantation has long remained the only definitive treatment for end-stage heart failure. Due to the limited organ supply, left ventricular assist devices (LVADs) have emerged as an additional treatment. LVADs were first approved as a "bridge to transplantation" but are increasingly being used as destination therapy [19, 20]. Exploiting the endogenous capability of cardiac regeneration could offer an additional option as well. There is renewed interest in utilizing stem cells to treat heart failure. Many clinical trials have shown positive effects of stem cell therapy in heart failure [21]. A recent meta-analysis

with 10 randomized-controlled trials demonstrated an increase in ejection fraction with concurrent reduction in left ventricular end-systolic and end-diastolic volumes [22]. However, the survival rate of delivered cells is very low, which suggest that these improvements are mainly caused by secretion of paracrine factors, and not by de novo cardiomyogenesis [23, 24]. Evidence suggests that these paracrine effects induce cardiomyocyte repair as well as possibly cardiomyocyte proliferation [25, 26].

Yes-associated protein (YAP) is a transcription factor that has been shown to promote heart regeneration [27]. It acts as a downstream regulator of the Hippo pathway, a kinase cascade implicated in regulating organ size. Through activation of Hippo, YAP is phosphorylated by Lats thereby excluding it from the nucleus and inactivating its role as a transcriptional activator. Alternatively, deactivation of Hippo leads to nuclear localization of unphosphorylated YAP. Unphosphorylated YAP interacts with other transcription factors such as TEAD, promoting cell-cycle re-entry and cell proliferation [28]. Chromatin immunoprecipitation sequencing (ChIP seq) in Hippo-deficient mice has shown that YAP directly affects not only cellular proliferation, but also cytoskeletal functions, such as cytoskeletal binding to extracellular matrix (ECM) though the Dystrophin glycoprotein complex (DGC) and F-actin polymerization [29]. Following apical resection, adult Hippo-deficient mice regenerated their hearts with characteristic cardiomyocyte protrusions of actin polymers. Furthermore, mice deficient in dystrophin, an essential component of the DGC, failed to regenerate their hearts after apical resection, although cell proliferation was unaffected. Together, this suggests that cardiomyocyte migration is dependent upon YAP-guided F-actin polymerization [29]. Intriguingly, unpublished work by Prof. Eldad Tzahor's group has shown that agrin associates with DGC, inducing its disassembly. This leads to sarcomeric disassembly and cell proliferation. Furthermore, injection of agrin into adult mice following apical resection led to restoration of ventricular function and increased cell proliferation, thereby suggesting that agrin is sufficient for heart regeneration. RT-qPCR measurements from endothelial cells, epicardium and cardiomyocytes within the apical thrombus showed that agrin expression was primarily confined to endothelial cells, and suggests that endothelial cells are responsible for agrin secretion. Finally, nuclear localization of YAP was increased in agrin-treated mice. The opposite role of DGC in proliferation and migration is intriguing and suggests that these are two independent pathways.

Recent studies using a rat and mouse model have shown that peripheral nerve regeneration after resection is dependent upon macrophage-induced angiogenesis between the two stumps of the transected nerve. The newly formed vessels form a bridge between the stumps, which Schwann cells use as a physical guide to regenerate axons. Initial angiogenesis is dependent upon macrophage secretion of VEGF-A. By blocking VEGF-A signaling in vivo (using VEGF-A antibody injection), angiogenesis and subsequent nerve regeneration was inhibited. Furthermore, by using VEGF-loaded beads as a decoy signal, axon growth could be diverted away from the distal stump and into nearby skeletal muscle [30].

We believe hearts regenerate in a similar manner to that of the peripheral nerve. A recent study demonstrated that macrophage-depletion impaired cardiac angiogenesis following MI and failed to regenerate despite preserved cardiomyocyte proliferation [31]. Therefore, we hypothesize that after apical resection, macrophages infiltrate the newly-formed apical thrombus and secrete cytokines such

as VEGF-A to stimulate angiogenesis to the resected region. Cardiomyocytes then migrate along the newly formed vessels to regenerate the ventricular apex.

Angiogenesis

In healthy tissue, *de novo* blood vessel formation can occur by three different mechanisms; vasculogenesis, sprouting angiogenesis and intussusception [32].

Vasculogenesis occurs in embryos. Three weeks into gestation, mesoderm-derived angioblasts in the human embryo coalesce to form a primitive vascular network. Factors from the Fibroblast Growth Factor (FGF) and Vascular Endothelial Growth Factor (VEGF) families are necessary for angioblast dedifferentiation.[33] Furthermore, endoderm-derived VEGF secretion is necessary for functional vascular formation and maintenance of angioblast differentiation [33]. Whether postnatal vasculogenesis occurs is controversial. Bone-marrow transplantation from transgenic mice in a mouse model of MI showed that transgenic endothelial progenitor cells (EPCs) contributed to the neovascularization at the infarct border [34]. This suggests that circulating, bone marrow-derived stem cells could be a cellular source for neovascularization. However, further analysis of EPCs implies that the cells are in fact not progenitors, but instead are monocytic cells with limited proliferative potential that stimulate angiogenesis through paracrine effects [35]. Further research using bone marrow transplants from GFP positive mice showed that bone-marrow derived cells did not incorporate into the endothelium, but instead filled the perivascular lining [36, 37]. Other publications have confirmed this finding, and showed that their angiogenic effects are mainly through paracrine secretion [38].

After initial vessel formation, further vascularization is mostly provided by sprouting angiogenesis. Many pathways, such as Angiopoietin, Notch, Wnt, TGFβ, FGF, Semaphorin, and Integrin signaling contribute to angiogenesis [39]. However, the principal angiogenic cytokine is arguably VEGF-A. In hypoxia, hypoxia-inducible factor-1 (HIF-1) stimulates VEGF-A expression [40]. In addition, a RNA-binding protein – named HuR – stabilizes VEGF mRNA, further contributing to its increased translation. During inflammation, migrating inflammatory cells contribute to the localized increase in VEGF-A. In response to increased cytokine and chemokine signaling, pericytes detach from the basement membrane by proteolytic cleavage mediated by matrix metalloproteases (MMPs). Concurrently, endothelial cells loosen their junctions and plasma proteins leak out into the extracellular matrix (ECM) to form a favorable foundation for new vessel outgrowth. Increased VEGF-A secretion induces competition between endothelial cells whereby the endothelial cell with the highest amount of DLL4 signaling (a Notch ligand) will become the leading migratory cell. The high amount of DLL4 signaling in this cell, termed the tip cell, changes its expression profile, and is characterized by increased PDGF-B, UNC5B, VEGFR2 and VEGFR3 expression, as well as extensive filopodia formation. The filopodia contain VEGFR2 and serve as chemokine sensors which drag the cell toward higher VEGF-A concentration. Concurrently, DLL4 from the tip cell suppresses the same transcriptional changes in adjacent cells. These cells, termed stalk cells, form adherens and tight junctions which keep the

migrating sprout intact. They are also responsible for forming a vascular lumen and maintaining luminal polarity. Eventually, migrating sprouts interconnect, endothelial cells become quiescent, and blood flow is established. Tissue inhibitors of matrix metalloproteases (TIMPs) and plasminogen activator inhibitor 1 (PAI-1) stimulate basement membrane deposition of the new vessel, which concurrently becomes covered in pericytes. As blood flow is essential for vessel sustainability, sprouts that fail to perfuse will regress [32, 39].

Intussusception is a process by which a vessel is cleaved in two by the ingrowth of endothelial cells. Through an increase in vessel wall shear stress, vessel walls from opposite sites protrude into the vascular lumen and merge forming a transluminal pillar. Later ingrowth of interstitial tissue and pericytes enlarges the pillar and ultimately splits the blood vessel [41]. Intussusception seems to play an important role in postnatal vascularization of the lung. During the first two years of life in humans, vascular density of the lung increases exponentially, necessitating more rapid vascularization then sprouting angiogenesis can provide [41, 42]. Evidence suggests that intussusception contributes to vascularization of the myocardium in early life as well [43]. Intussusception mostly occurs in capillaries and microvessels but has been observed in larger vessels as well [44].

Once a vessel is formed, endothelial cells acquire a perivascular layer. For capillaries and other microvessels, this layer consists of pericytes, while larger vessels form a perivascular smooth muscle layer which is termed the tunica media. Origin of the smooth muscle layer is complex. The dorsal aorta is the first great vessel to form and it's smooth muscle cells (SMCs) are derived from transdifferentiated endothelial cells [45]. The medial layer of the great thoracic arteries and proximal coronary arteries are derived from the neural crest, while the distal coronary arteries are of epicardial origin [45]. Migration of smooth muscle progenitors is directed by PDGF-B, secreted from immature or growing endothelial cells. Upon contact with the endothelial cells, the smooth muscle progenitors differentiate and form the perivascular layer [46, 47]. Similarily, PDGF-B has been shown to attract pericytes to the perivascular layer of microvessels [46].

Adult SMCs seem to either stem from proliferation of preexisting SMCs or bone-marrow derived progenitor cells. In models of heterotypic heart or aortic transplants, it has been shown that the majority of SMCs in the neointima of donor coronaries and aortas are host-derived [48, 49]. Additionally, by grafting β-galactosidase positive bone marrow into an irradiated aortic allograft, researchers showed that part of the aortic neointima consisted of β-galactosidase positive SMCs [50]. Together, these results support the conclusion that adult SMCs are in part derived from bone marrow-derived stem cells.

Hemodynamic forces have long been considered to be the main driving force of arterial or venous differentiation. However, evidence suggests that endothelial cell fate is determined as early as the migratory stage of angioblasts during embryologic vasculogenesis. Using a zebrafish model, researchers demonstrated that angioblasts in the lateral posterior mesoderm were destined to attain arterial or venous endothelial cell fates. This is regulated through Gridlock, a downstream regulator of Notch, which induces the arterial fate by suppressing venous formation [51].

However, grafting veins to the arterial circulation has shown that veins are able to remodel and form arterial-like vessels; they exhibit a thicker tunica media and tighter intercellular junctions [52].

Intriguingly, grafting a pulmonary valve in place of the aortic valve leads to the expression of EphB2 in valvular endothelial cells, an arterial marker [53]. This suggests considerable vascular plasticity, with vessels seemingly able to adapt to changes in environmental forces.

It is well described that if an arterial occlusion develops gradually, collateral arteries are able to compensate through vessel remodeling. This process is termed arteriogenesis. Arterial occlusion increases pulsatile shear stress of collateral vessels, thereby inducing nitric oxide (NO) synthesis in the endothelium. NO increases MCP-1 secretion from EC and SMCs, a well-known monocyte chemoattractant. Monocyte accumulation around the vessel leads to proteasa-mediated degradation of the internal elastic lamina and ECM, thereby providing room for vessel remodeling. ECs proliferate and increase the vessel diameter while SMCs form circular layers around the vessel, thereby increasing the thickness of the medial layer [54].

The formation of *de novo* arteriogenesis through capillary maturation has been suggested but its occurrence is debated [54, 55]. Arteriogenesis following occlusion of the internal iliac artery occurs with little variation in collateral positioning between individuals [54]. Similarily, the preexisting collateral network of vessels going through arteriogenesis following femoral occlusion has been well described in rabbits and mice without detection of *de novo* arteries [56, 57]. This suggests that *de novo* collateral arteries do not form following arterial occlusion.

Objectives

Since the initial report of the transient regenerative potential of the mammalian heart in 2011, the capacity of mammalian hearts to regenerate has been debated [7, 58]. Therefore, we first set out to see if the mammalian heart regenerates. Thereafter, we began to explore our hypothesis of vessel-directed cardiomyocyte migration. We investigated if vessel ingrowth precedes cardiomyocyte migration after apical resection, if migrating cardiomyocytes are in close proximity to vessels in the apical thrombus, and if cardiomyocytes migrate along endothelial cells in vitro. Lastly, we wanted to see if in vitro cardiomyocyte migration could be stimulated by a single chemotactic agent.

Materials and Methods

Animal handling

All animals were treated in accordance with the Guide for the Care and Use of Laboratory Animals (National Institutes of Health), and the procedures were approved by the Stanford University Animal Care and Use Committee (protocol 28921).

Apical resection

Resections of the ventricular apex of neonatal mice were performed as described previously [59]. Briefly, one day old CD-1 mice (P1) (*delivered from pregnant CD-1 mice (Charles River Laboratories)*) were subjected to apical resection or sham-operation. Neonates were anesthetized by hypothermia on an ice bed for 5 min. Hypothermia induces apnea and asystole which prevents excessive blood loss during surgery. The neonates were then transferred to the operating area and put in a supine position. The chest was sterilized with Betadine and a transverse skin incision was made. A lateral thoracotomy was performed through a small incision in the fourth intercostal space to expose the ventricular apex. The apex was subsequently resected gradually until the left ventricular cavity was exposed. A 6-0 suture and was used to close the chest wall and skin in separate layers. Neonates were then warmed rapidly and any remaining blood was cleaned to minimize risk of maternal cannibalization. All neonates were removed from the mother directly before surgery and returned together afterwards. This further reduces the risk of cannibalization.

Heart explants

Neonates were euthanized by decapitation. P5 and older mice were anesthetized with Isoflurane prior to decapitation. Following decapitation, the chest cavity was exposed via median sternotomy and the heart was explanted.

In vivo injections

For cell proliferation measurements, EdU labeling was performed using Click-iT® Imaging Kit (Invitrogen) according to the manufacturer's instructions. Briefly, EdU was injected intraperitioneally 12 hours before cardiac explant. EdU positivity was assessed with immunohistochemistry.

For assessment of vessel perfusion, lectin conjugated to a far-red fluorophore, was injected into the right ventricle of anesthetized mice 2 minutes before cardiectomy.

Primary antibodies

The following primary antibodies were used for immunohistochemistry staining at the indicated dilutions: α-smooth muscle actin (1:200, Abcam ab7817 and ab5694), sarcomeric α-actinin (1:200, Abcam ab9465), troponin I (1:200, Abcam ab56357), and VE Cadherin (1:600, Abcam ab33168).

Immunostaining

Neonatal hearts were explanted, rinsed with phosphate buffered saline (PBS) and embedded in OCT before being frozen in dry ice. 10 µm sagittal sections were then obtained using a cryostat (Thermo Scientific, CryoStar NX70).

Sections were fixed in 4% paraformaldehyde for 10 min, permeabilized in PBS containing 0.5% Tween for 15 min, and then blocked in 10% fetal bovine serum (FBS) for 1 hour at room temperature. Next, primary antibodies diluted in PBS were added and incubated for 1.5 hours at 37°C. Appropriate secondary antibodies diluted in PBS at 1:200 were then added and incubated for 45 min at 37°C. Finally, nuclear staining was performed using DAPI (Life Technologies) or Hoechst 33342 (Invitrogen). Sections were washed in PBS three times between each step. EdU labelling was performed using Click-iT® Imaging Kit (Invitrogen) according to the manufacturer's instructions.

For whole mount staining, neonatal hearts were explanted, rinsed with PBS and then put into 4% PFA for 1 hour before washing three times in PBS containing 0.2% Triton X-100 (PBS-Tx) for 10 min. Primary antibodies diluted in 0.2% PBS-Tx were added and allowed to incubate on a rocker at 4°C for 48 hours. Thereafter, hearts were washed three times in 0.2% PBS-Tx for 10 min each and then every 2 hours for the rest of the day. The next day, secondary antibodies, diluted in 0.2% PBS-Tx, and DAPI were added and allowed to incubate on a rocker at 4°C for 48 hours Subsequently, hearts were washed three times in 0.2% PBS-Tx and every 2 hours thereafter for the rest of the day. The next day, hearts were put in Vectashield (Vector Laboratories) and imaged.

Masson's trichrome staining

Frozen sections were acquired as described before. Sections were thawed for 20 min at 4° and then rinsed in 100% ethanol before being fixed in Bouin's solution for 3 hours at room temperature. Excess stain was then rinsed off in running water until water ran clear. Slides were then stained in Briebrich Scarlet-Acid Fuchsin before being washed in running water for 2 min Thereafter, slides were stained in Phosphotungstic/Phosphomolybdic Acid solution for 15 min and Aniline Blue solution for 20 min. Next, slides were placed in 1% acetic acid solution for 5 min before being rinsed in running water for 2 min. Lastly, slides were dehydrated in 95% ethanol, 100% ethanol and xylene for 2 min each. Cytoseal™ 60 (Richard-Allan Scientific) was used to attach slides to cover slips.

Confocal imaging and analysis

Confocal images were obtained using a Zeiss LSM 780 confocal microscope and Zen imaging software. The area of the resected apex was imaged using the tile scan feature. This meant that the same number of z-stacks and same acquisition settings were used for each sample and each experiment. Finally, maximum intensity projection of the z-stacks was acquired using Fiji software.

Blood vessel, smooth muscle, and fibrosis area measurements were obtained using Fiji software. For vessel and smooth muscle measurements, the thrombus area was selected and the signal of interest isolated. Images were then converted to 8-bit greyscale TIFF, thresholded, and made binary. Lastly, the area was measured using the measurement function. For fibrosis area measurements, the apical

area was selectively cropped. Thereafter, the color threshold function was used to automatically select and measure the whole apical area first, and then the fibrotic area only. The fibrotic area was calculated by dividing the size of the fibrotic area by the size of the heart.

Distance measurements between cardiomyocyte processes and the nearest blood vessel in the resected apex were manually obtained using Fiji software.

Cardiomyocyte isolation

Cardiomyocyte isolation was performed using the Pierce Primary Cardiomyocyte Isolation Kit (Thermo Scientific) according to the manufacturer's instructions. Briefly, hearts from P1-P3 mice were explanted as described before under sterilized conditions. Atria were removed from the explanted hearts and placed in 500 µL ice cold Hanks' balanced salt solution (HBSS). Ventricles were then minced into 1-3 mm^3 pieces using long scissors. Next, hearts were washed in ice cold HBSS twice for 5 min and centrifuged briefly at full speed in between. Thereafter, HBSS was aspirated and 200 µL of digestive enzyme solution 1, containing papain, and 10 µL of digestive solution 2, containing thermolysin, were added. Cells were allowed to incubate at 37°C for 35 min before being washed twice for 5 min in ice cold HBSS. Cells were centrifuged briefly at full speed in between. HBSS was aspirated and Dulbecco's modified eagle media (DMEM) containing 10% FBS was added. Finally, cell yield and viability was determined using trypan blue staining with a hemocytometer.

Transwell migration assay

A 24 well plate was coated with 100 µL of matrigel per well and allowed to incubate at 37°C for 1 hr. Thereafter, 25,000 human umbilical vein endothelial cells (HUVECs) were plated onto the matrigel and incubated for 12 hours at 37°C to allow tubules to form. Next, 25,000 green fluoroscent protein (GFP) positive cardiomyocytes were seeded onto the tubules. Images were acquired every 10 minutes over 12 hours using time-lapse microscopy.

Statistical analysis

All data are presented as mean ± SEM unless otherwise specified. The Wilcoxon test was used to compare differences between two groups. The Kruskal Wallis test was used to compare difference between multiple groups. The Conover test with Bonferroni correction was used as a post hoc test. All statistical tests were two-tailed and a P value less than 0.05 was considered significant. P values are indicated by asterisks as follows: * = $p<0.05$, ** = $p<0.01$, *** = $p<0.001$.

Results

The Murine Heart Regenerates With Minimal Fibrosis

After apical resection, a thrombus quickly forms to seal the cut edge and prevent exsanguination (Fig. 1, A and D). Over time, the thrombus organizes and by day 11 after surgery it becomes fibrotic (Fig 1, B and E). Gradually, the fibrotic area is replaced by myocardium; by day 30 the heart has regenerated with minimal fibrosis (Fig. 1, C and F). Quantification of the fibrotic area in the apex from day 11 to day 30 post-resection shows that fibrosis significantly decreases over the time ($p=0.011$) (Fig. 2A). Sham hearts were significantly less fibrotic than hearts 11 ($p=0.0016$) and 14 ($p=0.0098$) days after resection. However, there was no significant difference in fibrosis between sham hearts and hearts explanted 21 and 30 days post-resection (Fig 2A).

To measure cell proliferation, EdU injections were performed 12 hours before explant to label proliferating cells within the heart. EdU positive cells were thereafter counted in both the apex and remote areas of the heart. To see if resected hearts were more proliferative than sham controls, we measured the ratio of EdU positive cells. Cardiomyocytes from day 3 and 11 post-resection were significantly more proliferative in both the apex and remote area compared to that of sham controls, while differences between day 2 and day 14 hearts were insignificant (Fig. 2B). Consistently, apices of resected hearts had significantly higher number of EdU positive cells compared to remote myocardium, while differences between day 2 and 14 were insignificant (Fig. 2C). This may suggest that the stimulus for cardiomyocyte proliferation takes time after resection, and is sustained for over 1 week.

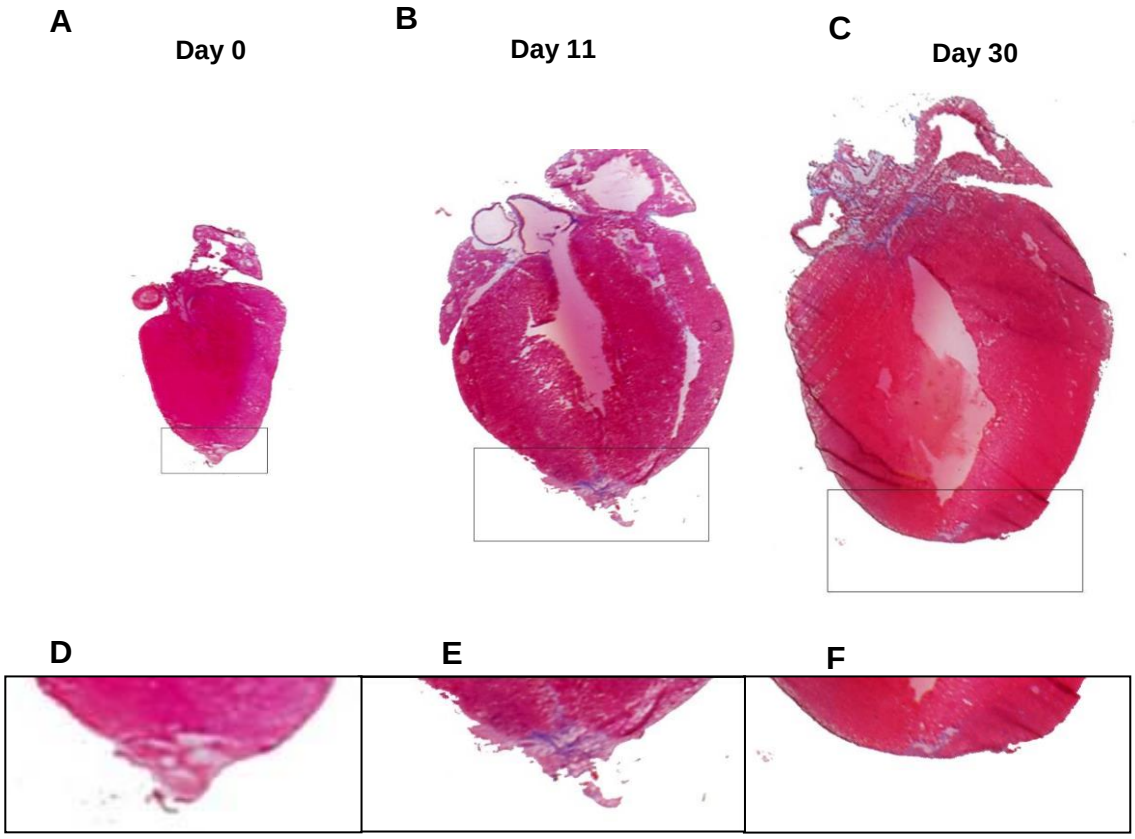

Figure 1: Masson's trichrome stained sections of apically resected hearts

A-C) Saggital heart sections day 0, 11, and 30 post-resection. D-F) Magnified images of boxed area from A-C).

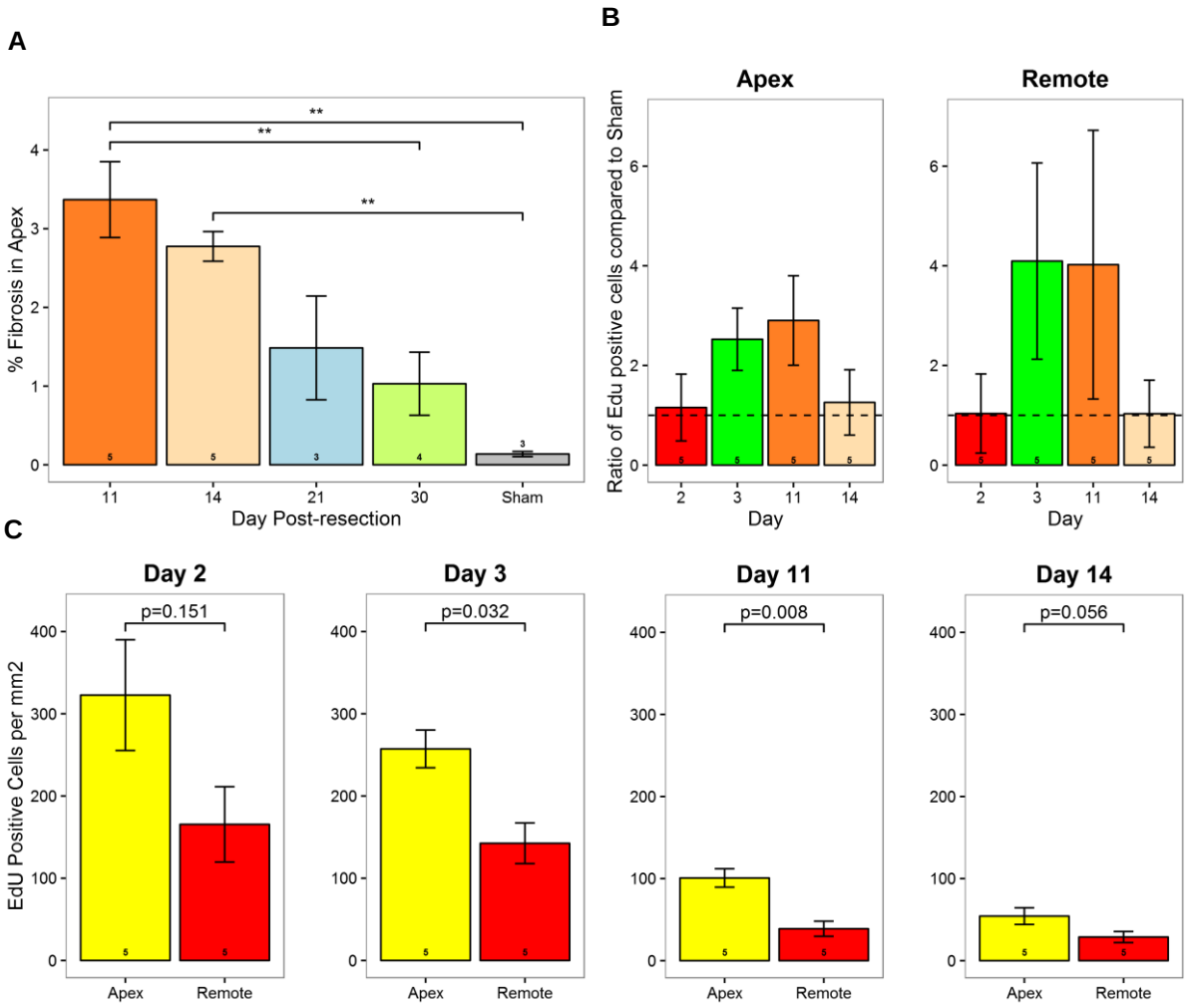

Figure 2: EdU and fibrosis measurements

A) Fibrotic area as a percent of myocardium within the apex at various time points after resection. B) EdU measurements comparing the number of proliferating cells in the apex and remote myocardium of resected hearts and sham controls. C) EdU measurements comparing the total number of proliferative cardiomyocytes in the apex and remote areas of resected hearts.

Vessel Ingrowth Precedes Cardiomyocyte Migration

In order to visualize revascularization of the apex following resection, and to see if blood vessel ingrowth precedes cardiomyocyte migration, immunohistochemical staining was performed and vessel density measurements of the resected region were performed using Fiji software. Numerous saggital sections of hearts from day 0 through day 21 post-resection were analyzed. In all sections, blood vessel ingrowth preceded cardiomyocyte migration. In fact, migrating vessels were first observed 2 days post-resection within the apical thrombus (Fig 3A). Arteries, characterized by a surrounding smooth muscle cell layer, developed within the thrombus in 1 of 5 hearts by 5 days post-resection (Fig 3B). By day 7 post-resection and onwards, all resected hearts contained true smooth-muscle cell-supported arteries in the region of thrombus (Fig 3C). Experiments with lectin perfusion revealed that blood vessels in the resected region become functional by day 5 post-resection (Fig. 3D). Using whole mount staining,

capillary plexus formation was observed in the apical thrombus, characteristic of vessel remodeling (Suppl. Fig. 1).

Vascular density continuously increased over time after apical resection ($p<0.001$), with numerous significant differences between individual time points (Fig. 4A). Similarly, smooth muscle density increased over time ($p=0.047$) with significant differences between day 5 and 11 ($p=0.022$) (Fig 4B). Lastly, maximal vessel diameter increased over time ($p=0.022$) (Fig 4C). The difference in maximal diameter was significantly increased for day 9 ($p=0.030$) and day 11 ($p=0.043$) when compared to day 5 (Fig. 4C). Together, endothelial cells invade the apical thrombus early and grow into functional arteries over time as part of the regenerative response.

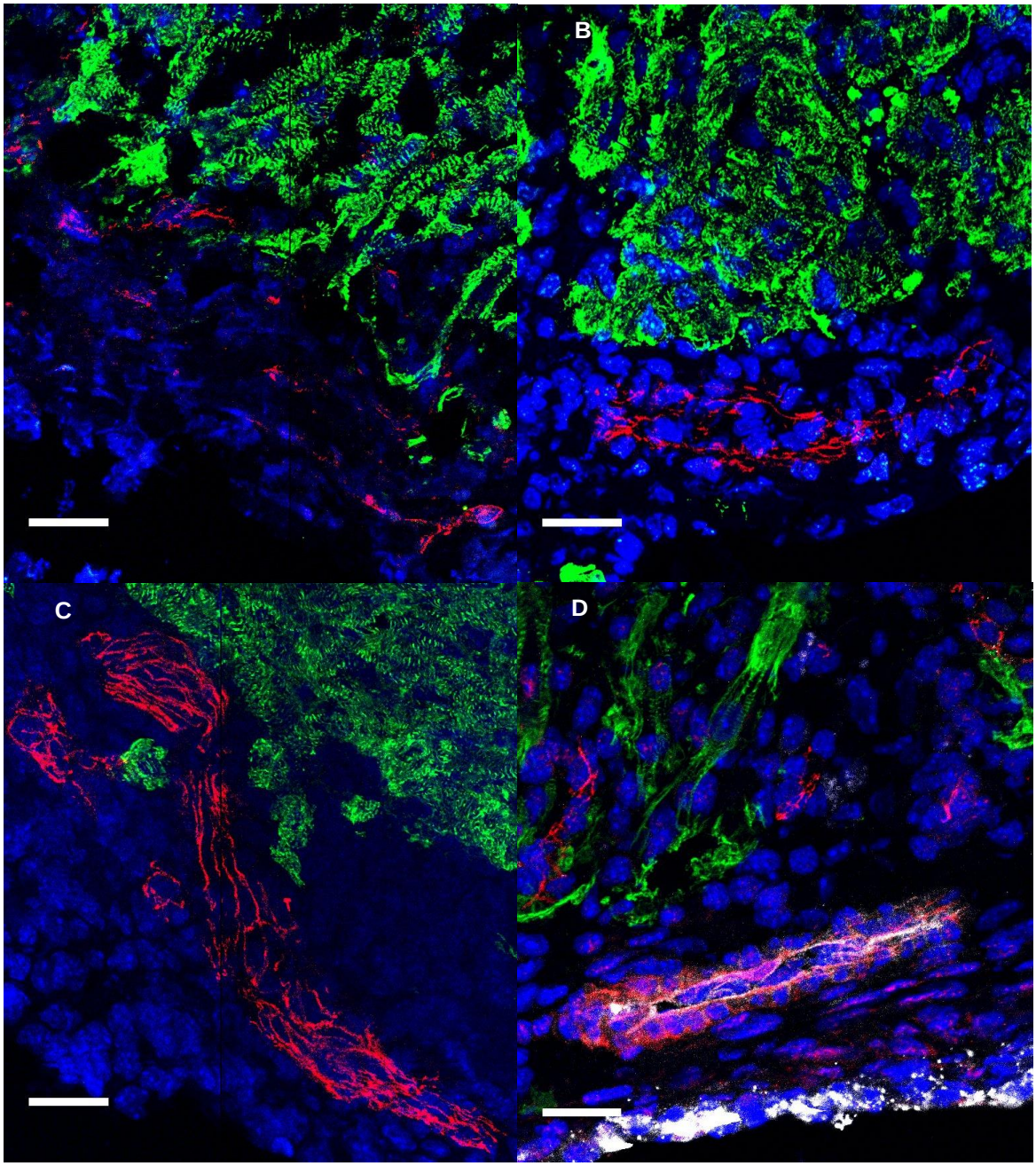

Figure 3: Representative images of vessel ingrowth into the apical thrombus after resection

Green = α-actinin, red = VE Cadherin (A and D) or SMA (B and C), blue = DAPI, white = Lectin (D), scale bar represents 25 µm.

A) Day 2 B) Day 5 C) Day 7 D) Day 5.

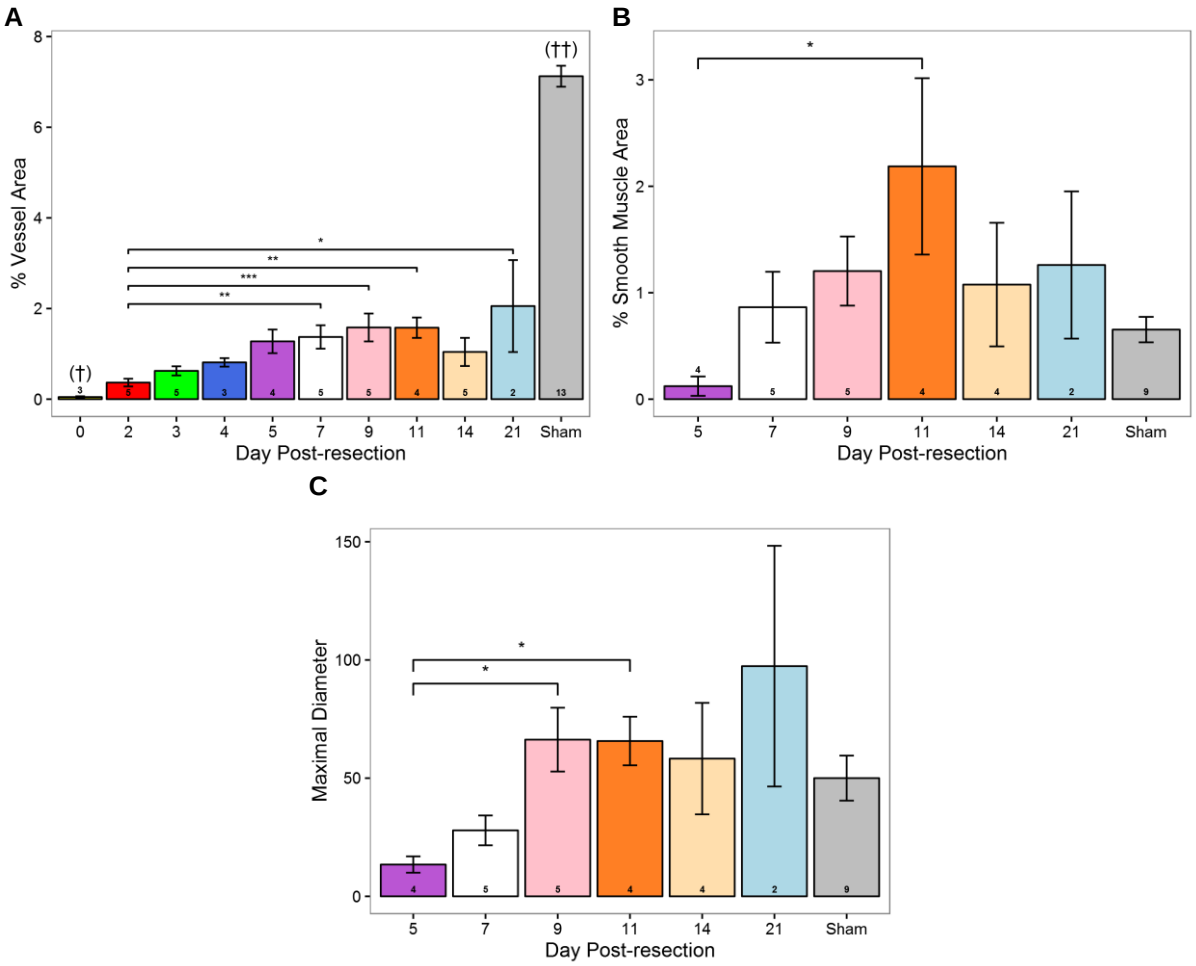

Figure 4: Quantification measurements of the apical thrombus

A) Vascular density. (†) Sham hearts were significantly more vascularized than hearts from day 0 (***), 2 (***), 3 (***), 4 (***), 5 (***), 7 (***), 9 (**), 11 (*) and 14 (***) post-resection. (††) Day 0 hearts were significantly less vascularized than hearts from day 5 (**), 7 (**), 9 (***), 11 (***), 14 (***) and 21 (***) post-resection; B) Percentage of smooth muscle cell area; C) Maximal vessel diameter.

Cardiomyocyte Processes Are In Close Proximity to Migrating Vessels

Cardiomyocyte processes, which are characteristic of migrating cardiomyocytes [29], were generally observed in close proximity to vessels in the apical thrombus (Fig 5). For quantification, the distance between the furthest part of a cardiomyocyte process and the nearest vessel in the apical thrombus were measured. Measurements from 215 cardiomyocyte processes showed that 69% of cardiomyocyte processes were within 15 µm of the nearest vessel, a distance representing the average diameter of 2 nuclei. The average distance between a cardiomyocyte process and its nearest blood vessel was 12.4 ± 0.9 µm.

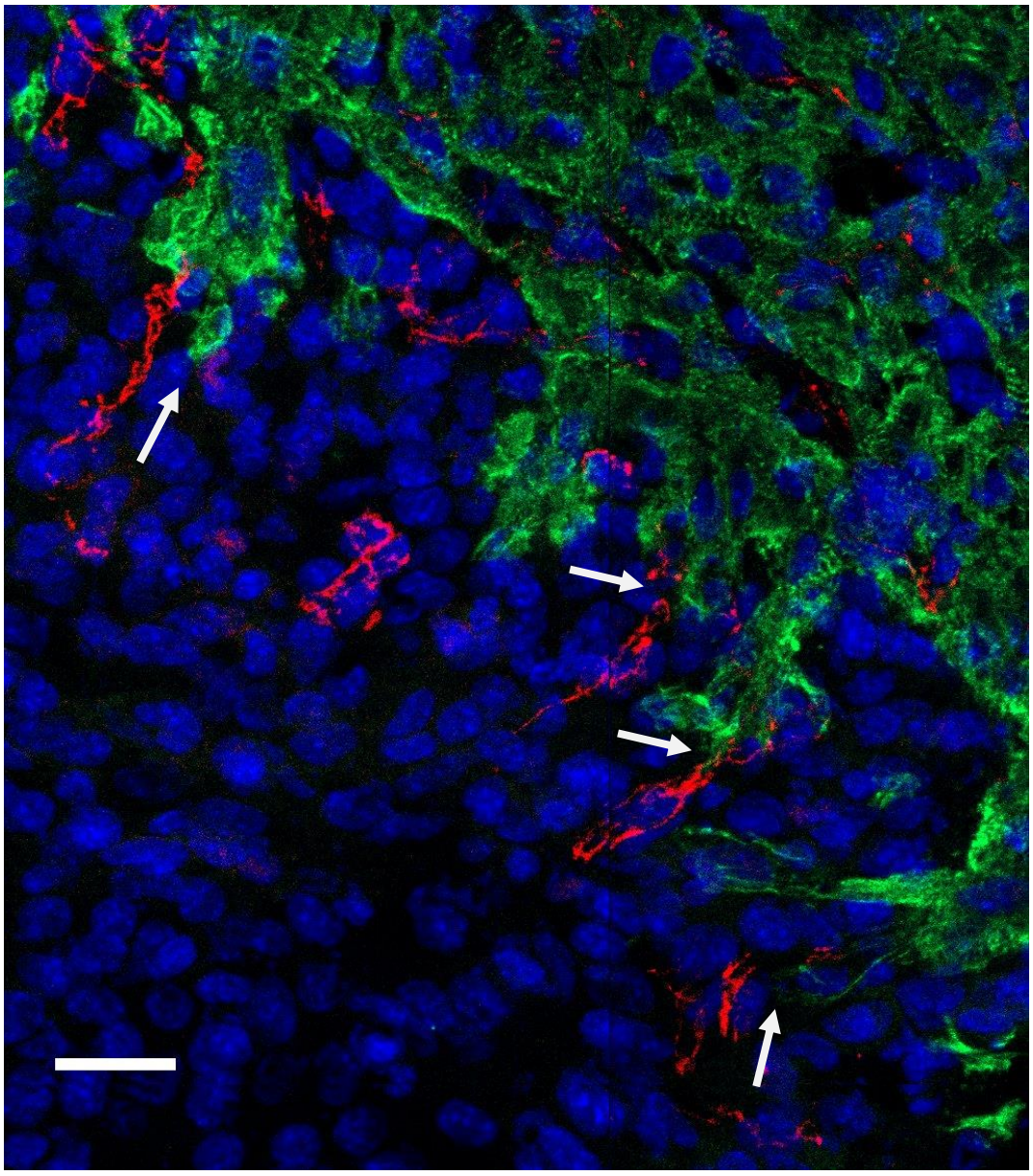

Figure 5: Close proximity of cardiomyocyte processes to blood vessels in the apical thrombus

IHC staining of apical thrombus 3 days post-resection. Note the close proximity of cardiomyocyte processes to migrating vessels in the apical thrombus (arrows). Green = α-actinin, red = VE cadherin, blue = Hoechst 33342

Cardiomyocytes Coalign With Endothelial Cells In Vitro

To address whether cardiomyocytes migrate along endothelial cells, murine GFP positive cardiomyocytes were co-cultured with human umbilical vein endothelial cells (HUVECs) *in vitro* and serial images were acquired using time-lapse microscopy. The majority of cardiomyocytes were found to coalign with the endothelial tubules. However, no cardiomyocyte migration was detected (Fig. 6).

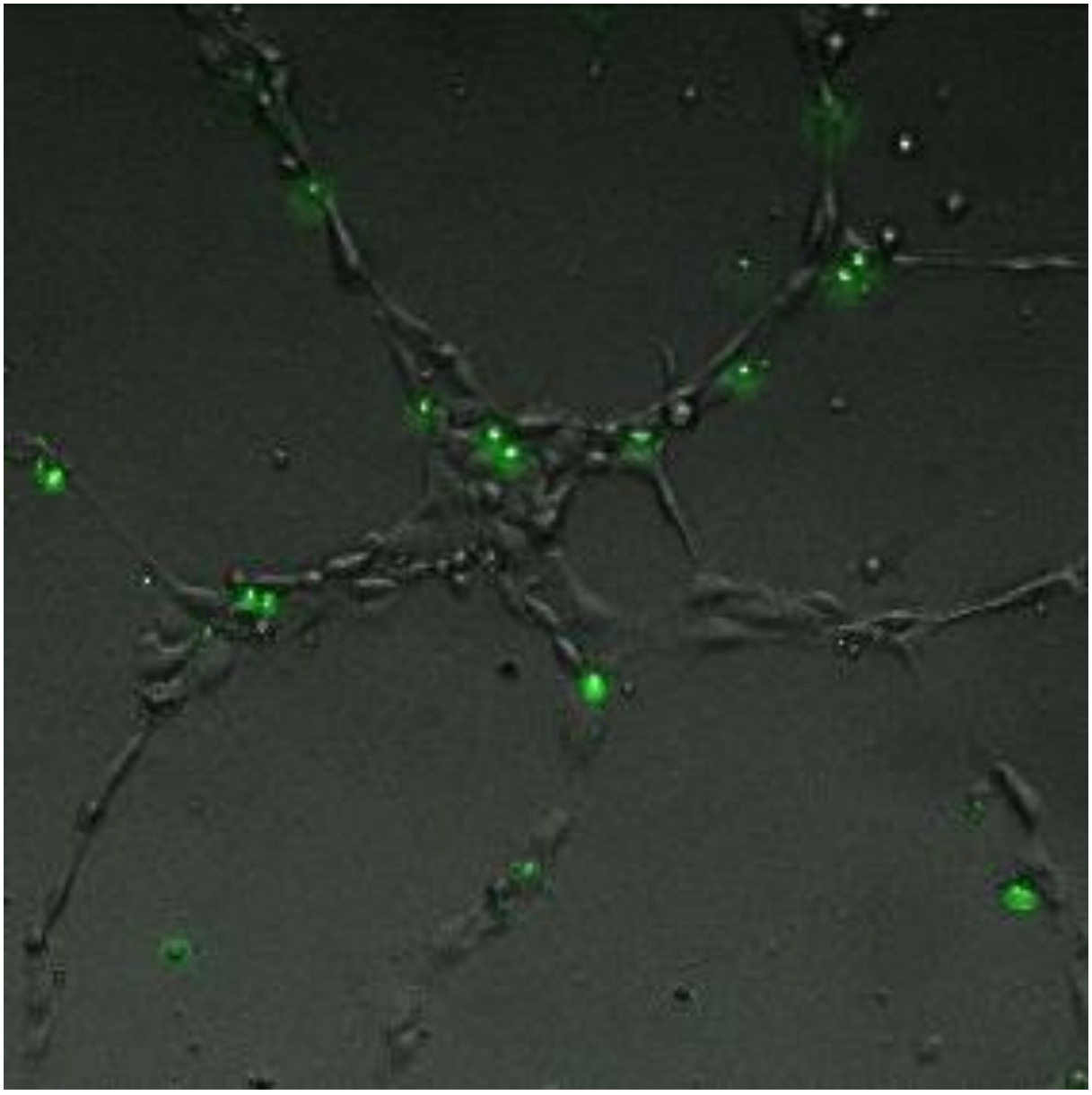

Figure 6: Cardiomyocytes co-cultured with HUVECs in vitro

Note the close proximity of cardiomyocytes (green) to the endothelial tubules.

Discussion

Masson's trichrome staining and EdU measurements suggest that the heart regenerates from pre-existing cardiomyocytes with minimal fibrosis; and this finding is consistent with previous reports [7]. For EdU measurements, 5 resected hearts and 1 sham were available from each time point. Ideally, more sham hearts should be added in order to draw conclusions about differences in the two groups. This, however, gives us a general idea that there is likely a true difference. Resected hearts from day 3 and 11 post-resection had a significantly higher number of EdU positive cells than sham hearts. However, differences between hearts at day 2 and 14 post-op were both non-significant. Consistently, apices of resected hearts were significantly more proliferative than remote areas at day 3 and 11 post-op. Differences at day 2 and 14 were insignificant. This suggests that cardiomyocyte proliferation is increased from day 3 through day 11. This may suggest that the stimulus for cardiomyocyte proliferation takes time after resection, and is sustained for over 1 week. More samples are needed for confirmation.

Immunohistochemical staining showed that blood vessels precede cardiomyocyte migration into the apical thrombus. Furthermore, the vascularity, maximal vessel diameter, and arterial maturation significantly increased within the resected region over time. The formation of larger arteries – characterized by a surrounding smooth muscle layer – within the apical thrombus by day 5 after resection is suggestive of *de novo* arteriogenesis. Microvessels appeared to remodel to form larger vessels. Interestingly, blood vessels are already perfused within 5 days of resection, suggesting that increased blood flow might stimulate vessel remodeling. This is consistent with arteriogenesis following arterial occlusion; sheer-stress from increased blood flow is responsible for collateral artery remodeling [54]. Additionally, hemodynamic forces in the mouse yolk sac has been shown to be both sufficient and necessary for vessel maturation [60].

The existence of *de novo* arteriogenesis has so far remained debated [54, 55]. Studies using arterial occlusion models have shown that collateral blood flow forms with little individual variation and without detection of *de novo* arteries [54, 56, 57]. Since no vessels were observed below the resection plane at day 0 (Suppl. Fig. 2) we conclude that all vessels in the apical thrombus at later timepoints are new. Our results are therefore highly suggestive of postnatal *de novo* arteriogenesis.

Our results demonstrated that the majority of migrating cardiomyocytes within the regenerating apex were in close proximity to blood vessels. However, some cardiomyocyte processes were noted to be present without adjacent blood vessels. IHC staining was performed on 10 µm sections, which is slightly thicker than the diameter of an average nucleus. Therefore, an explanation why some migrating cardiomyocytes did not appear near a blood vessel could be that the blood vessels are simply out of viewing plane. Whole mount staining, which permits 3-dimensional visualization of the explanted heart, might clarify whether all migrating cardiomyocytes are in close proximity to blood vessels. Additionally, electron microscopy of the apical region would help confirm whether there is direct cell contact between cardiomyocytes and endothelial cells.

Using a transwell migration assay with 10% FBS as the chemoattractant, we demonstrated that the majority of cardiomyocytes coaligned with endothelial tubules. No migration occurred however. The basis for migration is attraction toward a higher chemokine gradient [61]. The lack of migration may be explained by the absence of a gradient across the transwell. The next step will be to run a migration assay where a chemokine gradient can be established. We are planning to use a microfluidics chamber. The chamber has numerous microchannels and a controllable chemical gradient is created across the chamber. Cell migration is then tracked using time-lapse microscopy.

Whether cardiomyocytes migrate directly along blood vessels requires further investigation. The close proximity of cardiomyocytes to blood vessels both *in vivo* and *In vitro* at least suggests a strong relationship between the two cell types. One possible explanation for the close proximity of cardiomyocytes to endothelial cells could be that blood vessels are the source of cardiomyocyte chemoattractants. This is consistent with our findings that blood vessels precede cardiomyocyte migration into the apical thrombus. Furthermore, endothelial cell chemokine secretion has been well described; for example, endothelial cells play a key role in leukocyte attraction during inflammation [62].

Alternatively, the close proximity between endothelial cells and cardiomyocytes may be attributable to a common chemoattractant that stimulates both cell types. While endothelial cell chemotaxis has been extensively described, little is known about cardiomyocyte chemotaxis. A study using ventricular amputation in zebrafish demonstrated that epicardial-derived SDF-1α induces cardiomyocyte migration [63]. Interestingly, the SDF-1a receptor, CXCR4b was expressed in cardiomyocytes but not endothelial cells. Furthermore, blocking the CXCR4b receptor resulted in defective cardiomyocyte migration without affecting the endothelial cells. This is in contrast to findings showing that CXCR4 is expressed in human endothelial cells [64, 65]. However, there are fundamental differences in the SDF signaling cascade of zebrafish and mammals. Zebrafish express two SDF isoforms, SDF-1α and SDF-1β, as opposed to mammals, which only express SDF-1α. Embryonic knockout of SDF-1α in mammals is lethal as SDF-1a plays a key role in embryologic development, such as blood vessel development and cell migration in organogenesis. In zebrafish however, this embryologic development seems to be mostly driven by the SDF-1β pathway, therefore knockout of SDF-1α is not lethal [63]. SDF-1α has been described as a chemoattractant for human umbilical vein endothelial cells *in vitro* [66]. This suggests that in mammals, SDF-1α may serve as a common chemoattractant for both cardiomyocytes and endothelial cells. If a common chemoattractant is indeed the case, then it is also important to identify the cell responsible for migratory signaling.

Based on data from prior studies, the epicardium may, in fact, drive cardiac regeneration. In our study, myocardium appeared to regenerate more robustly along the epicardial edges before regenerating deeper myocardium (Suppl. Fig. 3). Additionally, it is well described that epicardial activation is a key factor in heart regeneration, and also is essential for cardiac development [67]. Epicardial cells exposed to retinoic acid *in vitro* secrete paracrine factors that induce cardiomyocyte proliferation. However, epicardial cells become less responsive to retinoic acid during the first week of postnatal life. Concurrently, cardiomyocytes lose the ability to respond to epicardial-derived paracrine

factors [68]. This is consistent with reports that mammalian hearts lose their regenerative potential after the first week of life [7].

Another possible source of cardiomyocyte and endothelial cell chemoattractants is macrophages. Macrophages are known to secrete VEGF, IGF-1 and TGF-β; factors that are linked to restoration of ventricular function and angiogenesis following cardiac injury [69]. In fact, macrophage depletion prevented neovascularization of the infarct region and prevented cardiac regeneration in neonatal mice [31]. We plan to assess whether macrophages are the predominant cell type within the apical thrombus by immunohistochemical staining for CD45 and F4/80.

The capacity for mammalian heart regeneration has only been known for 5 years, and many questions remain unanswered. The dystrophin glycoprotein complex (DGC) has been shown to be essential for cardiomyocyte migration. Interestingly, dystrophin-deficient neoanates fail to regenerate after apical resection although cell proliferation is unaffected, suggesting cardiomyocyte proliferation and migration are directed by two separate mechanisms [29]. We believe apical resection as an ideal model to study both cardiomyocyte migration and vessel maturation. Heart injury models such as acute coronary ligation and cryoinjury leads to necrosis and intramyocardial inflammation that can harm regenerative responses in adjacent healthy tissue. Resection, on the other hand, removes tissue with a minimal inflammatory response in nearby myocardium. Additionally, visualization of ingrowing cells is optimal as the apical thrombus within the resected region is easily distinguishable from overlying myocardium.

References

1. Poss, K.D., L.G. Wilson, and M.T. Keating, *Heart Regeneration in Zebrafish.* Science, 2002. **298**(5601): p. 2188-2190.
2. Witman, N., et al., *Recapitulation of Developmental Cardiogenesis Governs the Morphological and Functional Regeneration of Adult Newt Hearts Following Injury.* Developmental Biology, 2011. **354**(1): p. 67-76.
3. Oberpriller, J.O. and J.C. Oberpriller, *Response of the Adult Newt Ventricle to Injury.* Journal of Experimental Zoology, 1974. **187**(2): p. 249-259.
4. Tam, S.K.C., et al., *Cardiac Myocyte Terminal Differentiation.* Annals of the New York Academy of Sciences, 1995. **752**(1): p. 72-79.
5. Li, F.Q., et al., *Rapid Transition of Cardiac Myocytes from Hyperplasia to Hypertrophy During Postnatal Development.* Journal of Molecular and Cellular Cardiology, 1996. **28**(8): p. 1737-1746.
6. Cole-Jeffrey, C.T., et al., *Progressive Anatomical Closure of Foramen Ovale in Normal Neonatal Mouse Hearts.* The Anatomical Record: Advances in Integrative Anatomy and Evolutionary Biology, 2012. **295**(5): p. 764-768.
7. Porrello, E.R., et al., *Transient Regenerative Potential of the Neonatal Mouse Heart.* Science, 2011. **331**(6020): p. 1078-1080.
8. Porrello, E.R., et al., *Regulation of Neonatal and Adult Mammalian Heart Regeneration by the miR-15 Family.* Proceedings of the National Academy of Sciences of the United States of America, 2013. **110**(1): p. 187-192.
9. Haubner, B.J., et al., *Functional Recovery of a Human Neonatal Heart After Severe Myocardial Infarction.* Circulation Research, 2016. **118**(2): p. 216-221.
10. Boulton, J., et al., *Survival After Neonatal Myocardial Infarction.* Pediatrics, 1991. **88**(1): p. 145-50.
11. Deutsch, M.A., et al., *Successful Management of Neonatal Myocardial Infarction with ECMO and Intracoronary r-tPA lysis.* Congenital Heart Disease, 2014. **9**(5): p. E169-E174.
12. Farooqi, K.M., et al., *Neonatal Myocardial Infarction: Case Report and Review of the Literature.* Congenital Heart Disease, 2012. **7**(6): p. E97-E102.
13. Murugan, S.J., J. Gnanapragasam, and J. Vettukattil, *Acute Myocardial Infarction in the Neonatal Period.* Cardiology in the Young, 2002. **12**(04): p. 411-413.
14. Peeters, S., et al., *Myocardial Infarction in a Neonate with Hereditary Antithrombin III Deficiency.* Acta Pædiatrica, 1993. **82**(6-7): p. 610-613.
15. Saker, D.M., et al., *Cardiac Recovery and Survival After Neonatal Myocardial Infarction.* Pediatric Cardiology, 1997. **18**(2): p. 139-142.
16. Bergmann, O., et al., *Evidence for Cardiomyocyte Renewal in Humans.* Science, 2009. **324**(5923): p. 98-102.
17. Mollova, M., et al., *Cardiomyocyte Proliferation Contributes to Heart Growth in Young Humans.* Proceedings of the National Academy of Sciences, 2013. **110**(4): p. 1446-1451.
18. Mill, J.G., et al., *Remodeling in the ischemic heart: the stepwise progression for heart failure.* Brazilian Journal of Medical and Biological Research, 2011. **44**(9): p. 890-898.
19. Xie, A., K. Phan, and T.D. Yan, *Durability of Continuous-Flow Left Ventricular Assist Devices: A Systematic rReview.* Annals of Cardiothoracic Surgery, 2014. **3**(6): p. 547-556.
20. Abraham, W.T. and S.A. Smith, *Devices in the Management of Advanced, Chronic Heart Failure.* Nature Reviews: Cardiology, 2013. **10**(2): p. 98-110.
21. Menasche, P., *Stem cells in the Management of Advanced Heart Failure.* Current Opinion in Cardiology, 2015. **30**(2): p. 179-185.
22. Kandala, J., et al., *Meta-Analysis of Stem Cell Therapy in Chronic Ischemic Cardiomyopathy.* The American Journal of Cardiology, 2013. **112**(2): p. 217-225.

23. Terrovitis, J.V., R.R. Smith, and E. Marbán, *Assessment and Optimization of Cell Engraftment After Transplantation Into the Heart.* Circulation Research, 2010. **106**(3): p. 479-494.
24. Mirotsou, M., et al., *Paracrine Mechanisms of Stem Cell Reparative and Regenerative Actions in the Heart.* Journal of Molecular and Cellular Cardiology, 2011. **50**(2): p. 280-289.
25. Garbern, Jessica C. and Richard T. Lee, *Cardiac Stem Cell Therapy and the Promise of Heart Regeneration.* Cell Stem Cell, 2013. **12**(6): p. 689-698.
26. Loffredo, Francesco S., et al., *Bone Marrow-Derived Cell Therapy Stimulates Endogenous Cardiomyocyte Progenitors and Promotes Cardiac Repair.* Cell Stem Cell, 2011. **8**(4): p. 389-398.
27. Xin, M., et al., *Hippo Pathway Effector Yap Promotes Cardiac Regeneration.* Proceedings of the National Academy of Sciences of the United States of America, 2013. **110**(34): p. 13839-44.
28. Yu, F.-X. and K.-L. Guan, *The Hippo Pathway: Regulators and Regulations.* Genes and Development, 2013. **27**(4): p. 355-371.
29. Morikawa, Y., et al., *Actin Cytoskeletal Remodeling with Protrusion Formation Is Essential For Heart Regeneration in Hippo-Deficient Mice.* Science Signaling, 2015. **8**(375): p. ra41-ra41.
30. Cattin, A.-L., et al., *Macrophage-Induced Blood Vessels Guide Schwann Cell-Mediated Regeneration of Peripheral Nerves.* Cell, 2015. **162**(5): p. 1127-1139.
31. Aurora, A.B., et al., *Macrophages Are Required for Neonatal Heart Regeneration.* Journal of Clinical Investigation, 2014. **124**(3): p. 1382-1392.
32. Carmeliet, P. and R.K. Jain, *Molecular Mechanisms and Clinical Applications of Angiogenesis.* Nature, 2011. **473**(7347): p. 298-307.
33. Risau, W., *Mechanisms of Angiogenesis.* Nature, 1997. **386**(6626): p. 671-674.
34. Asahara, T., et al., *Bone Marrow Origin of Endothelial Progenitor Cells Responsible for Postnatal Vasculogenesis in Physiological and Pathological Neovascularization.* Circulation Research, 1999. **85**(3): p. 221-228.
35. Rehman, J., et al., *Peripheral Blood "Endothelial Progenitor Cells" Are Derived From Monocyte/Macrophages and Secrete Angiogenic Growth Factors.* Circulation, 2003. **107**(8): p. 1164-1169.
36. Rajantie, I., et al., *Adult Bone Marrow-Derived Cells Recruited During Angiogenesis Comprise Precursors for Periendothelial Vascular Mural Cells.* Blood, 2004. **104**(7): p. 2084-2086.
37. Ziegelhoeffer, T., et al., *Bone Marrow-Derived Cells Do Not Incorporate Into the Adult Growing Vasculature.* Circulation Research, 2004. **94**(2): p. 230-238.
38. Pearson, J.D., *Endothelial Progenitor Cells – Hype or Hope?* Journal of Thrombosis and Haemostasis, 2009. **7**(2): p. 255-262.
39. Phng, L.K. and H. Gerhardt, *Angiogenesis: A Team Effort Coordinated by Notch.* Developmental Cell. **16**(2): p. 196-208.
40. Forsythe, J.A., et al., *Activation of Vascular Endothelial Growth Factor Gene Transcription by Hypoxia-Inducible Factor 1.* Molecular and Cellular Biology, 1996. **16**(9): p. 4604-4613.
41. Burri, P.H., R. Hlushchuk, and V. Djonov, *Intussusceptive Angiogenesis: Its Emergence, Its Characteristics, and Its Significance.* Developmental Dynamics, 2004. **231**(3): p. 474-488.
42. Zeltner, T.B., et al., *The Postnatal Development and Growth of the Human Lung. I. Morphometry.* Respiration Physiology, 1987. **67**(3): p. 247-267.
43. van Groningen, J.P., A.C.G. Wenink, and L.H.M. Testers, *Myocardial Capillaries: Increase in Number by Splitting of Existing Vessels.* Anatomy and Embryology, 1991. **184**(1): p. 65-70.
44. Djonov, V.G., H. Kurz, and P.H. Burri, *Optimality in the Developing Vascular System: Branching Remodeling by Means of Intussusception As An Efficient Adaptation Mechanism.* Developmental Dynamics, 2002. **224**(4): p. 391-402.
45. Carmeliet, P., *Manipulating Angiogenesis in Medicine.* Journal of Internal Medicine, 2004. **255**(5): p. 538-561.

46. Hellstrom, M., et al., *Role of PDGF-B and PDGFR-beta in Recruitment of Vascular Smooth Muscle Cells and Pericytes During Embryonic Blood Vessel Formation in the Mouse.* Development, 1999. **126**(14): p. 3047-3055.
47. Hirschi, K.K., S.A. Rohovsky, and P.A. D'Amore, *PDGF, TGF-β, and Heterotypic Cell–Cell Interactions Mediate Endothelial Cell–induced Recruitment of 10T1/2 Cells and Their Differentiation to a Smooth Muscle Fate.* The Journal of Cell Biology, 1998. **141**(3): p. 805-814.
48. Hillebrands, J.-L., et al., *Origin of Neointimal Endothelium and α-actin–Positive Smooth Muscle Cells in Transplant Arteriosclerosis.* The Journal of Clinical Investigation. **107**(11): p. 1411-1422.
49. Saiura, A., et al., *Circulating Smooth Muscle Progenitor Cells Contribute to Atherosclerosis.* Nature Medicine, 2001. **7**(4): p. 382-383.
50. Shimizu, K., et al., *Host Bone-Marrow Cells are a Source of Donor Intimal Smooth- Muscle-Like Cells in Murine Aortic Transplant Arteriopathy.* Nature Medicine, 2001. **7**(6): p. 738-741.
51. Zhong, T.P., et al., *Gridlock Signalling Pathway Fashions the First Embryonic Artery.* Nature, 2001. **414**(6860): p. 216-220.
52. Kwei, S., et al., *Early Adaptive Responses of the Vascular Wall during Venous Arterialization in Mice.* The American Journal of Pathology, 2004. **164**(1): p. 81-89.
53. Rabkin-Aikawa, E., et al., *Clinical Pulmonary Autograft Valves: Pathologic Evidence of Adaptive Remodeling in the Aortic Site.* The Journal of Thoracic and Cardiovascular Surgery, 2004. **128**(4): p. 552-561.
54. Schaper, W., *Collateral Circulation.* Basic Research in Cardiology, 2009. **104**(1): p. 5-21.
55. Carmeliet, P., *Mechanisms of Angiogenesis and Arteriogenesis.* Nature Medicine, 2000. **6**(4): p. 389-395.
56. Scholz, D., et al., *Ultrastructure and Molecular Histology of Rabbit Hind-Limb Collateral Artery Growth (Arteriogenesis).* Virchows Archiv, 2000. **436**(3): p. 257-270.
57. Wagner, S., et al., *Magnetic Resonance Angiography of Collateral Vessels in a Murine Femoral Artery Ligation Model.* NMR in Biomedicine, 2004. **17**(1): p. 21-27.
58. Konfino, T., et al., *The Type of Injury Dictates the Mode of Repair in Neonatal and Adult Heart.* Journal of the American Heart Association, 2015. **4**(1).
59. Mahmoud, A.I., et al., *Surgical Models for Cardiac Regeneration in Neonatal Mice.* Nature Protocols, 2014. **9**(2): p. 305-311.
60. Lucitti, J.L., et al., *Vascular Remodeling of the Mouse Yolk sac Requires Hemodynamic Force.* Development, 2007. **134**(18): p. 3317-3326.
61. Devreotes, P.N. and S.H. Zigmond, *Chemotaxis in Eukaryotic Cells: A Focus on Leukocytes and Dictyostelium.* Annual Review of Cell Biology, 1988. **4**(1): p. 649-686.
62. Johnston, B. and E.C. Butcher, *Chemokines in Rapid Leukocyte Adhesion Triggering and Migration.* Seminars in Immunology, 2002. **14**(2): p. 83-92.
63. Itou, J., et al., *Migration of Cardiomyocytes Is Essential for Heart Regeneration in Zebrafish.* Development, 2012. **139**(22): p. 4133-4142.
64. Gupta, S.K., et al., *Chemokine Receptors in Human Endothelial Cells Functional Expression of cxcr4 and Its Transcriptional Regulation by Inflammatory Cytokines.* Journal of Biological Chemistry, 1998. **273**(7): p. 4282-4287.
65. Salvucci, O., et al., *Regulation of Endothelial Cell Branching Morphogenesis by Endogenous Chemokine Stromal-Derived Factor-1.* Blood, 2002. **99**(8): p. 2703-2711.
66. Mirshahi, F., et al., *SDF-1 Activity on Microvascular Endothelial Cells.* Thrombosis Research. **99**(6): p. 587-594.
67. Masters, M. and P.R. Riley, *The Epicardium Signals the Way Towards Heart Regeneration.* Stem Cell Research, 2014. **13**(3, Part B): p. 683-692.
68. Chen, T.H.P., et al., *Epicardial Induction of Fetal Cardiomyocyte Proliferation via a Retinoic Acid-Inducible Trophic Factor.* Developmental Biology, 2002. **250**(1): p. 198-207.

69. Kennedy-Lydon, T. and N. Rosenthal, *Cardiac Regeneration: Epicardial Mediated Repair.* Proceedings of the Royal Society of London B: Biological Sciences, 2015. **282**(1821).

Supplemental Information

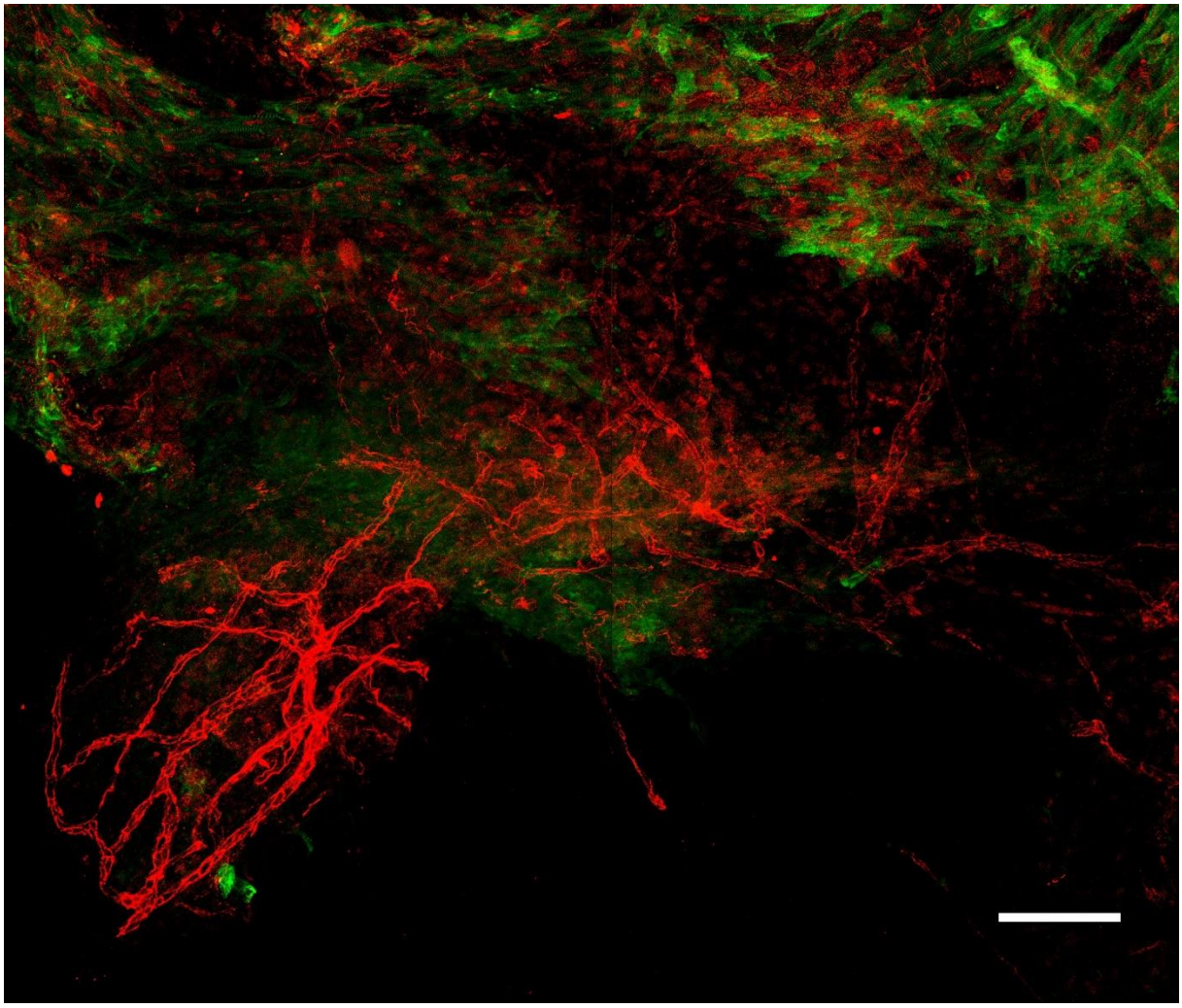

Supplementary Figure 1: Vessel remodeling in the apical thrombus

Whole mount staining of a heart 7 days post-resection. Note the remodelling capillary plexus below the myocardial border. α-actinin = green, red = VE Cadherin. Scale bar respresents 100 µm.

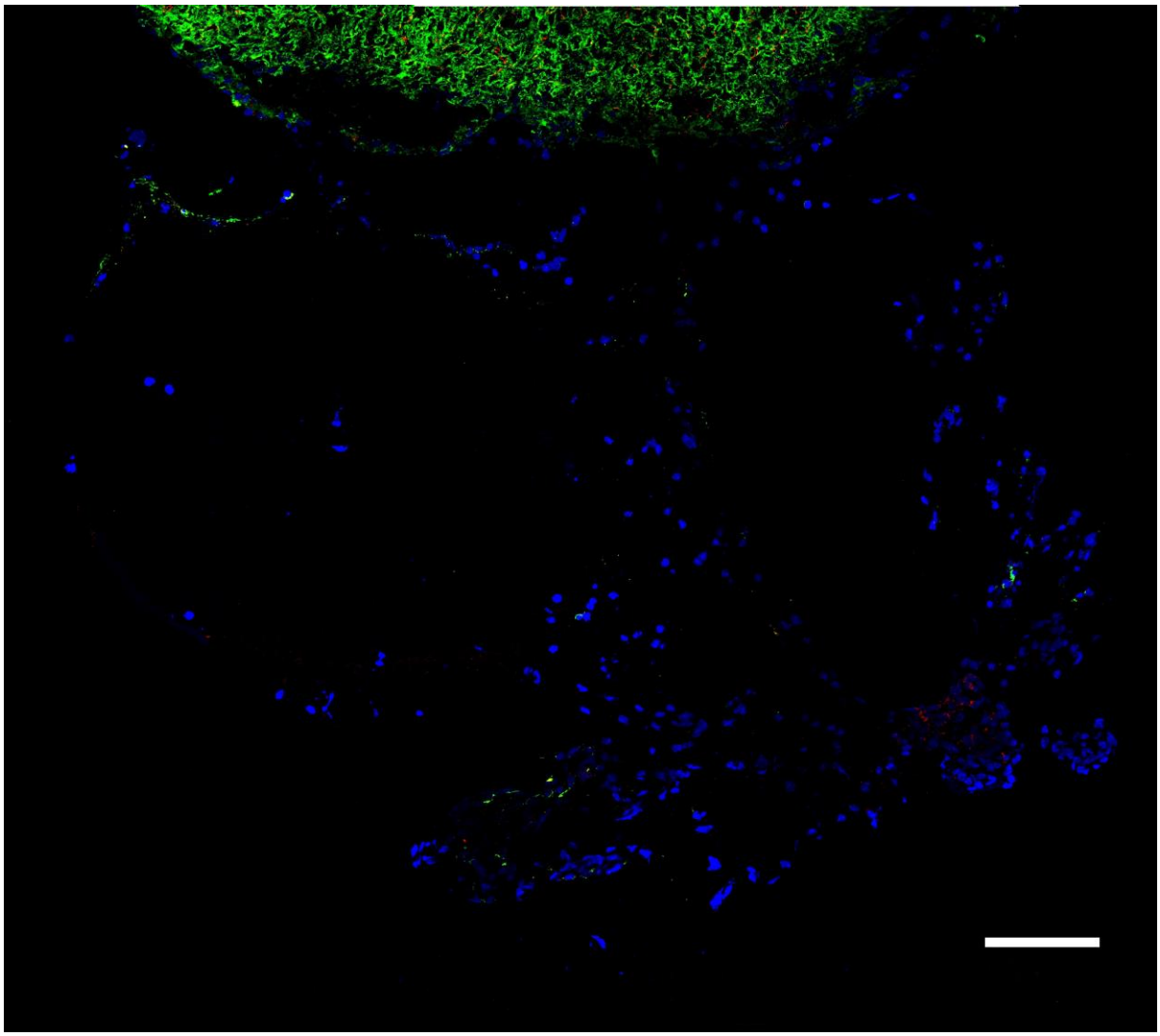

Supplementary Figure 2: IHC staining of a heart day 0 post-resection

Note the absence of blood vessels in the apical thrombus, below the resection plane. Additionally, nuclei are sparse as this likely precedes influx of hematopoietic cells. α-actinin = green, red = VE Cadherin, blue = DAPI. Scale bar respresents 100 µm.

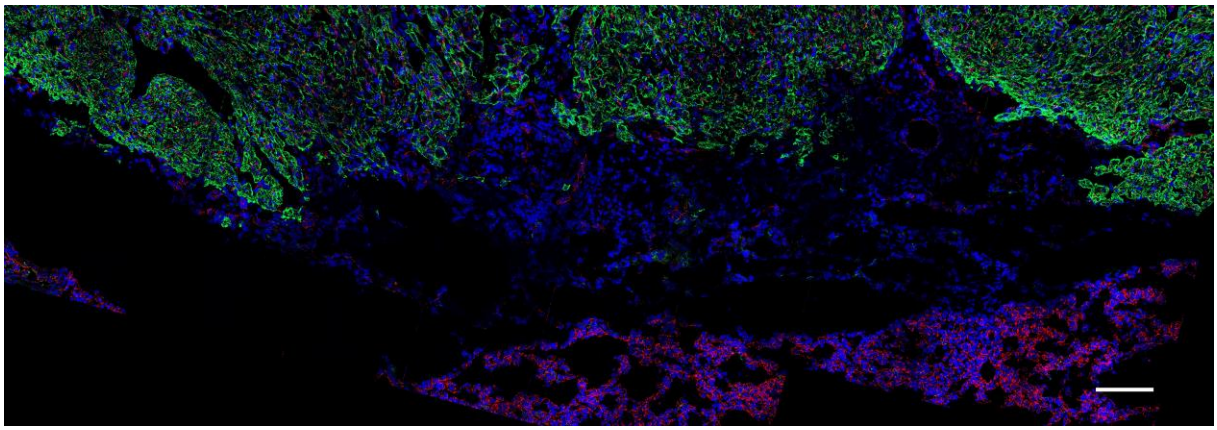

Supplementary Figure 3: Myocardium follows along the epicardial border

Above is a representative tissue section from a heart 14 days after apical resection. Note how migration along the epicardial border is more prominent than in the middle of the section. The highly-vascular tissue at the bottom of the figure is the adjacent lung. α-actinin = green, red = VE Cadherin, blue = DAPI. Scale bar respresents 100 µm.